NAVAL POSTGRADUATE SCHOOL
Monterey, California

THESIS

PROPAGATION SPEEDS OF OCEAN SURFACE WAVES IN SHALLOW WATER

by

Nick A. Sarap Jr.

March 1999

Thesis Advisor:	T.H.C. Herbers
Second Reader:	E.B. Thornton

Approved for public release; distribution is unlimited.

REPORT DOCUMENTATION PAGE

Form Approved
OMB No. 0704-0188

Public reporting burden for this collection of information is estimated to average 1 hour per response, including the time for reviewing instruction, searching existing data sources, gathering and maintaining the data needed, and completing and reviewing the collection of information. Send comments regarding this burden estimate or any other aspect of this collection of information, including suggestions for reducing this burden, to Washington headquarters Services, Directorate for Information Operations and Reports, 1215 Jefferson Davis Highway, Suite 1204, Arlington, VA 22202-4302, and to the Office of Management and Budget, Paperwork Reduction Project (0704-0188) Washington DC 20503.

1. AGENCY USE ONLY *(Leave blank)*	2. REPORT DATE March 1999	3. REPORT TYPE AND DATES COVERED Master's Thesis

4. TITLE AND SUBTITLE PROPAGATION SPEEDS OF OCEAN SURFACE WAVES IN SHALLOW WATER	5. FUNDING NUMBERS
6. AUTHOR(S) Sarap, Nick A. Jr.	

7. PERFORMING ORGANIZATION NAME(S) AND ADDRESS(ES) Naval Postgraduate School Monterey, CA 93943-5000	8. PERFORMING ORGANIZATION REPORT NUMBER

9. SPONSORING / MONITORING AGENCY NAME(S) AND ADDRESS(ES)	10. SPONSORING / MONITORING AGENCY REPORT NUMBER

11. SUPPLEMENTARY NOTES

The views expressed in this thesis are those of the author and do not reflect the official policy or position of the Department of Defense or the U.S. Government.

12a. DISTRIBUTION / AVAILABILITY STATEMENT Approved for public release; distribution is unlimited.	12b. DISTRIBUTION CODE

13. ABSTRACT *(maximum 200 words)*

Nonlinear effects on the dispersion relation of waves in shallow water are examined with measurements collected on a mild sloping sandy beach during the recent Sandy Duck experiment. Four arrays of bottom pressure sensors were deployed in depths ranging from 3 – 6 m during August-November, 1997. For each of these arrays, a root-mean-square average wavenumber was estimated as a function of frequency from the cross-spectra of one-hour-long pressure records. The observed wavenumbers are compared to linear finite depth theory predictions and to predictions based on a stochastic formulation of weakly nonlinear Boussinesq equations that incorporate both frequency and amplitude dispersion effects. The observed wavenumbers are generally in agreement with the nonlinear theory predictions and deviate significantly (maximum errors averaged over the spectrum of about 25%) from the linear theory predictions. In high energy conditions with breaking or nearly breaking waves, the effects of amplitude and frequency dispersion tend to cancel, and all components of the wave spectrum travel with approximately the shallow water wave speed. These results are consistent with previous studies.

14. SUBJECT TERMS Nearshore Processes, Surf Zone, Waves			15. NUMBER OF PAGES 52
			16. PRICE CODE

17. SECURITY CLASSIFICATION OF REPORT Unclassified	18. SECURITY CLASSIFICATION OF THIS PAGE Unclassified	19. SECURITY CLASSIFI- CATION OF ABSTRACT Unclassified	20. LIMITATION OF ABSTRACT UL

NSN 7540-01-280-5500

Standard Form 298 (Rev. 2-89)
Prescribed by ANSI Std. 239-18

i

PROPAGATION SPEEDS OF OCEAN SURFACE WAVES IN SHALLOW WATER

Nick A. Sarap Jr.
Lieutenant, United States Navy
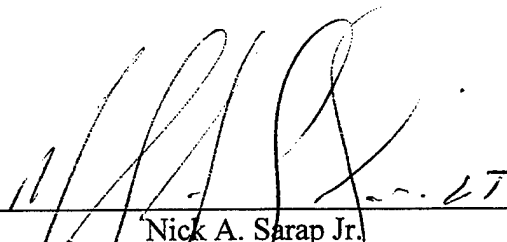B.S. Bethany College, 1991

Submitted in partial fulfillment
of the requirements for the degree of

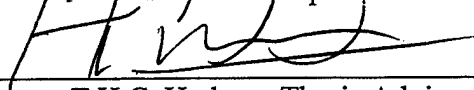## MASTER OF SCIENCE IN PHYSICAL OCEANOGRAPHY

from the

NAVAL POSTGRADUATE SCHOOL
March 1999

Author: _____
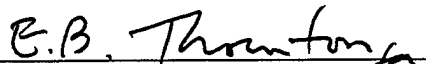Nick A. Sarap Jr.

Approved by: _____
T.H.C. Herbers, Thesis Advisor

_____
E.B. Thornton, Second Reader

_____
R.W. Garwood, Chairman
Department of Oceanography

ABSTRACT

Nonlinear effects on the dispersion relation of waves in shallow water are examined with measurements collected on a mild sloping sandy beach during the recent Sandy Duck experiment. Four arrays of bottom pressure sensors were deployed in depths ranging from 3 – 6 m during August-November, 1997. For each of these arrays, a root-mean-square average wavenumber was estimated as a function of frequency from the cross-spectra of one-hour-long pressure records. The observed wavenumbers are compared to linear finite depth theory predictions and to predictions based on a stochastic formulation of weakly nonlinear Boussinesq equations that incorporate both frequency and amplitude dispersion effects. The observed wavenumbers are generally in agreement with the nonlinear theory predictions and deviate significantly (maximum errors averaged over the spectrum of about 25%) from the linear theory predictions. In high energy conditions with breaking or nearly breaking waves, the effects of amplitude and frequency dispersion tend to cancel, and all components of the wave spectrum travel with approximately the shallow water wave speed. These results are consistent with previous studies.

TABLE OF CONTENTS

ACKNOWLEDGMENTS

I.   INTRODUCTION

As surface gravity waves approach the beach their characteristics change
dramatically. During shoaling, wave heights increase, wavelengths decrease, and
propagation directions refract toward normal incidence to the beach. These linear
propagation effects are well understood. In very shallow water strong nonlinear effects
dominate the wave shoaling evolution. The nonlinear interaction between two wave
components with frequencies and (vector) wavenumbers (f_1, k_1) and (f_2, k_2) can transfer
energy to a wave component with the sum frequency and wavenumber $(f_1 + f_2, k_1 + k_2)$.
Whereas these so-called triad interactions are non-resonant in deep water, the mismatch
from resonance is small in shallow water, causing large energy transfers over distances of
only a few wavelengths. Subsequent interactions involving the newly formed waves can
transfer energy to even higher frequencies. As a result the wave spectrum typically
broadens during shoaling (e.g. Freilich & Guza, 1984). Furthermore, phase-coupling
effects between the interacting wave components causes the characteristic steepening and
pitching forward of wave crests that leads in to wave breaking (Elgar & Guza, 1985).

The basis for wave shoaling theory are equations for weakly nonlinear and weakly
dispersive waves derived by Boussinesq in 1871. This theory has turned out to be
suprisingly accurate even for nearly breaking waves. Peregrine (1967) extended the
Boussinesq theory to a sloping bottom, and the resulting equations were used by Freilich
and Guza (1984) to model the shoaling evolution of irregular ocean waves on a gently
sloping beach. This model predicts accurately the evolution of both the wave spectrum

1

E(f) and wave shape characteristics observed on natural beaches (Freilich & Guza, 1984; Elgar & Guza, 1985).

Nonlinearity affects not only the spectral properties of waves but also the dispersion relation between the wave frequency *f* and the wavenumber $k = (| \boldsymbol{k} |)$. In the linear approximation

$$(2\pi f)^2 = gk \tanh(kh) \tag{1}$$

where *h* is the water depth and *g* is gravity. Equation 1 is valid in any depth *h*, but neglected nonlinear effects may distort the dispersion relation. In deep ($kh \gg 1$) and intermediate ($kh = O(1)$) water depths, observed dispersion relations are generally in excellent agreement with (Eq. 1) at the dominant wind wave frequencies, whereas at higher frequencies observed spectra are often dominated by bound waves excited by nonresonant triad interactions that have wavenumbers *k* much smaller than predicted by (Eq. 1) (e.g. Donelan et al., 1985; Herbers & Guza, 1992, 1994). Freilich and Guza (1984) examined nonlinear deviations from (Eq. 1) in shallow water ($kh \ll 1$) by comparing wave phase evolution across the beach with linear theory predictions, based on (Eq. 1) and nonlinear predictions based on Boussinesq models for uni-directional waves. In low energy conditions with a broad-banded wave field, linear phase prediction was more accurate than the Boussinesq model predictions, possibly because the latter are inaccurate in deep water and neglect directional effects. However, in energetic wave conditions with narrow spectra, large errors were noted in the linear phase predictions at frequencies corresponding to harmonic peaks in the spectra, whereas the nonlinear model

predictions are in good agreement with the observations. Elgar and Guza (1985) compared wave phase speeds, estimated from measured phase differences between closely spaced sensors in a cross-shore array, to predictions of linear finite depth theory and a nonlinear Boussinesq model. As in the Freilich and Guza (1984) study, the nonlinear model predictions assume uni-directional waves. The nonlinear model predictions are generally in closer agreement with the data than the linear model, and demonstrate that high-frequency harmonic components in narrow banded wave fields travel with the same (or slightly larger) speeds than the dominant swell components

In a weakly nonlinear wave field, the wavenumber of each spectral component is affected by nonlinear triad interactions with other components of the spectrum. As a result there is no unique dispersion relation between f and k. However, the root-mean-square average wavenumber of all wave components with frequency f can be expressed in terms of the spectra $E_{\eta_x}(f)$ and $E_{\eta_y}(f)$ of the sea surface slopes η_x and η_y in two orthogonal (x,y) directions (e.g. Herbers & Guza,1994).

$$k_{rms}(f) = \left(\frac{E_{\eta_x}(f) + E_{\eta_y}(f)}{E(f)} \right)^{1/2} \qquad (2)$$

A theoretical expression for $k_{rms}(f)$, that is generally valid for directionally spread waves propagating over a beach that is uniform in the alongshore direction, can be derived from a stochastic formulation of Boussinesq equations (Herbers & Burton ,1997, Herbers et al., 1999, manuscript in preparation).

$$k_{rms}(f) = k_{sw}(f)\left[1 + \varepsilon_{fr}(f) - \varepsilon_{am}(f)\right]^{1/2} \qquad (3)$$

3

The lowest-order term of (Eq. 3), $k_{sw}(f) = 2\pi f / \sqrt{gh}$, is the well-known shallow water

limit of (Eq. 1), that describes a nondispersive wave field in which all components of the

wave spectrum travel with the shallow water wave speed $\sqrt{gh}$. The small correction

terms $\varepsilon_{fr}(f)$ and $\varepsilon_{am}(f)$ represent the effects of frequency dispersion and amplitude

dispersion. The frequency dispersion correction is obtained by expanding the tanh (kh)

term in (Eq.1) in a Taylor series for small kh

$$\varepsilon_{fr}(f) = \frac{(2\pi f)^2 h}{3g} \tag{4}$$

that describes the linear dispersion effect of wave speeds to decrease with increasing

frequency The amplitude dispersion correction is given by:

$$\varepsilon_{am}(f) = \frac{3}{2hE(f)} \left\{ \int_0^f \operatorname{Re}\{B(f', f - f')\}df' + 2\int_0^\infty \operatorname{Re}\{B(f', f)\}df' \right\} \tag{5}$$

where Re{ } indicates the real part. The bispectrum $B(f_1, f_2)$ describes in a statistical sense

the nonlinear interaction between triads of wave components with frequencies f_1, f_2 and

f_1+f_2, and the associated nonlinear phase changes of the three components (e.g. Elgar &

Guza, 1985; Herbers & Burton, 1997). The net nonlinear changes in the wavenumber of

components with frequency f are obtained by integrating the contributions of all triad

interactions that involve a component with frequency f In general, larger amplitude

waves propagate faster (i.e. have smaller wavenumbers) than smaller amplitude waves,

and thus the amplitude dispersion term $\varepsilon_{am}(f)$ tends to negate the frequency dispersion

term $\varepsilon_{fr}(f)$. Equations 3 - 5 are based on the standard Boussinesq assumption that

dispersion $(kh)^2$ and nonlinearity a/h are both weak and of the same order (that is, the

Ursell number $U_r = a/k^2h^3 = O(1)$). Hence the frequency $\varepsilon_{fr}(f)$ and amplitude

$\varepsilon_{am}(f)$ dispersion correction terms in (Eq. 3) are formally of the same order.

In the present study the dispersion properties of waves in shallow water are examined with field data acquired during the SandyDuck experiment near Duck, NC. Four arrays of bottom pressure sensors were deployed for four months along a cross-shore transect on a sandy beach. These measurements provide unique detailed wavenumber estimates both inside and outside the surf zone. The field experiment and data analysis techniques are described in Chapter II. Comparisons of the predicted and the observed wavenumbers for four case studies, including both breaking and non-breaking waves are carried out in Chapter III. Statistical analysis of the entire data set is performed in Chapter IV. The results are summarized in Chapter V.

6

II.   FIELD EXPERIMENT AND DATA ANALYSIS

Detailed measurements of the shoaling evolution of waves across the beach were collected during the SandyDuck experiment at the U.S. Army Corps of Engineer's Field Research Facility located near Duck, NC, on a straight barrier island that is fully exposed to the Atlantic Ocean. An extensive 2-dimensional array of pressure sensors, electromagnetic current meters, and sonar altimeters (to determine seafloor location) were deployed on the beach between the shoreline and about 6 m depths (Elgar et al; manuscript in preparation). High quality wave data were collected during a four-month period (August – December 1997) spanning a wide range of conditions.

Bathymetry at the site is characterized by a gently sloping ($\approx$1:250), nearly planar inner shelf and a slightly steeper ($\approx$1:100) beach with a steep (1:20) beach face (Fig. 1). Daily bathymetric surveys of the nearshore region indicate that the beach changes over the course of the experiment were small. A shore-parallel sand bar located 300 m offshore remained relatively stationary with its crest submerged about 5 m below sea level, and did not strongly affect the wave shoaling process. Close to shore, the morphology was more dynamic, with the development of transient bars and alongshore depth variations.

The present study uses data from four compact arrays, each consisting of six bottom-mounted pressure sensors (Fig. 1) arranged in two-dimensional formations. The arrays were positioned at offshore distances of 210, 260, 385, and 500 m in nominal

7

depths of 3, 3.5, 4, and 5 m, respectively with sensor spacings ranging from 4 – 12 m (Fig. 2). The shortest lags in the arrays are small compared to the wavelengths of the dominant waves, and thus allow for accurate estimates of surface slopes in two orthogonal directions η_x and η_y (Herbers & Guza, 1994). The sample frequency of the pressure sensors was 2 Hz.

The data analysis is based on 1-hour-long detided bottom pressure records. Spectra, cross-spectra, and bispectra were estimated in the frequency range of 0 – 0.5 Hz with a bandwidth of 0.0098 Hz.

An estimate of $\hat{k}_{rms}(f)$ is obtained from a linear combination of the normalized cross spectra (Herbers, Elgar, & Guza, 1995)

$$\hat{k}_{rms}^{2}(f) = \sum_{p=1}^{N_i}\sum_{q=1}^{N_i}\alpha_{pq}\frac{H_{pq}(f)}{\left[H_{pp}(f)H_{qq}(f)\right]^{1/2}} \tag{6}$$

where $H_{pq}(f)$ is the cross spectrum of a pair of sensors with indices p and q and N_i is the number of sensors in the array. The method, valid for arbitrary directional wave spectra, is based on an expansion of the cross spectra $H_{pq}(f)$ for small values of kD, where D is the sensor spacing (see Herbers et al, 1995 for details). The optimal coefficients α_{pq} are evaluated *a priori* through a least-squares fit of the expanded right-hand-side of (Eq. 6) to the theoretical expression for $k_{rms}(f)$, (Eq. 2).

Boussinesq model predictions of $k_{rms}(f)$, (Eq. 3-5), were obtained by substituting measured spectra $(E(f))$ and bispectra $(B(f_1,f_2))$, extracted from the bottom pressure time

8

series, in (Eq. 5). To enhance the stability of the estimates, both $E(f)$ and $B(f_1,f_2)$ were averaged over the six sensors of each array. The weak (in the Boussinesq approximation) vertical attenuation of wave pressure over the water column is neglected in these calculations. The frequency range for comparisons of wavenumber estimates was restricted to $0.05 - 0.25$ Hz because both the Boussinesq model and the data analysis techniques do not account for the typically strong reflections of lower-frequency (< 0.05 Hz) infragravity waves from shore, and higher frequency (> 0.25 Hz) waves are significantly attenuated over the water column at the deeper arrays.

III. OBSERVATIONS

In this chapter, example comparisons of observed and predicted wavenumbers are presented. Four case studies were selected from a wide range of conditions encountered during the four month-long experiment (Fig. 3). Three of the selected data runs, (cases II-IV), were collected during the passage of major storms through the region. In these case studies with energetic (significant wave heights H_s >2 m) waves propagating and breaking across the instrumented transect, the nonlinear effects on the dispersion relation are expected to be pronounced. The results are contrasted with one data run (case I) collected in generic calm conditions.

Observed spectra ($E(f)$) and observed and predicted root-mean-square average wavenumbers $k_{rms}(f)$ are shown for each individual case study in Figs. 4 – 7. In particular, the observed $k_{rms}(f)$ (Eq. 2) are compared to both the linear dispersion relation (Eq. 1) and the $k_{rms}(f)$ predicted by the nonlinear Boussinesq model (Eq.3). To examine the relative importance of the frequency ($\varepsilon_{fr}(f)$) and amplitude ($\varepsilon_{am}(f)$) dispersion correction terms in the nonlinear Boussinesq model prediction, the wavenumbers predicted by the shallow water dispersion relation approximation ($k_{sw}(f)$ i.e. excluding both $\varepsilon_{fr}(f)$ and $\varepsilon_{am}(f)$ in Eq. 3) and by the dispersion relation of the linearized Boussinesq model (excluding only $\varepsilon_{am}(f)$ in Eq. 3) are included in Figs. 4 - 7.

11

In each of the four case studies, one of the arrays had one or more malfunctioning instruments and was not included in the comparisons presented in Figs. 4 - 7.

Case I. NOVEMBER 20

The conditions on November 20 are characterized by light winds (speeds < 5 m/s) and a fairly broad spectrum of low amplitude swell with a peak frequency $f_p \approx 0.07$ Hz (Fig. 4a), The surf zone was confined to the region shoreward of the shallowest array. The offshore significant wave height was 0.3 m and the mean wave direction was 12° south of normal incidence (both measured with a Datawell Directional Waverider in 20 m depth, 5 km from shore). The small increases in variance observed between arrays 7 and 5 (9%) and between arrays 5 and 4 (19%) in Fig. 4a are consistent with the theoretical ($\propto h^{-1/2}$) energy increase of nonbreaking waves expected during shoaling (e.g. Kinsman, 1965). Observed wavenumbers are generally in good agreement with linear finite depth theory (Figs. 4b-d), but there is a slight but systematic discrepancy at higher frequencies at all arrays. The nonlinear Boussinesq model predictions agree well with the observed $k_{rms}(f)$ frequencies. Whereas the nonlinear Boussinesq model prediction of $k_{rms}(f)$ is close to the linear Boussinesq predictions (i.e. $\varepsilon_{am}(f)$ is small compared to $\varepsilon_{fr}(f)$, Eq. 3) at array 7, at array5 the nonlinear Boussinesq prediction is close to $k_{sw}(f)$ (i.e. $\varepsilon_{am}(f)$ and $\varepsilon_{fr}(f)$ approximately cancel). Although these results demonstrate primarily the linearity of the wave motion in benign conditions, amplitude dispersion effects are detectable at the shallowest array where nonlinearity is enhanced. Whereas predicted $k_{rms}(f)$ vary smoothly with frequency, the observed $k_{rms}(f)$ show some scatter

12

at low frequencies. These discrepancies are possibly caused by errors in the observed wavenumbers. Previous observations at the same field site have shown that wave reflection from shore is significant at low swell frequencies when incident wave amplitudes are small (Elgar et al., 1994). The resulting partial standing wave patterns likely contribute significant errors to $k_{rms}(f)$ estimates that are based on the assumption of a progressive wave field.

Case II. NOVEMBER 7

A much more energetic and narrower swell spectrum ($f_p \approx 0.08$ Hz) was observed on November 7 (Fig. 5a). At the deeper arrays, (6, 7), the observed spectra have a distinct 2nd harmonic peak at $2f_p \approx 0.16$ Hz. The offshore significant wave was 2.28 m and the mean-direction was close to normal incidence. Local winds were variable with speeds less than 10 m/s, indicating that the swell arrived from a remote source. Observed swell variances decreased by 17% between arrays 7 and 6 and by 43% between arrays 6 and 5, indicating that significant dissipation took place in the instrumented region with surf zone conditions extending seaward of array 5 (Fig. 5a). At all three arrays, the observed $k_{rms}(f)$ are in good agreement with the linear finite depth theory at the dominant swell frequencies but diverge gradually from the linear dispersion relation for f ≥ 0.15 Hz. At the highest frequency considered (0.25 Hz) the observed $k_{rms}(f)$ are about 25% smaller than the wavenumbers predicted by the linear finite depth dispersion relation (Figs. 5b-d). These discrepancies at high frequencies ($\geq 2f_p$) are consistent with harmonic components with smaller wavenumbers. The nonlinear Boussinesq model predictions

13

(that account for the harmonic components) are in excellent agreement with the observed wavenumbers over the entire frequency range. Both the observed $k_{rms}(f)$ and the nonlinear Boussinesq prediction are close to the shallow water dispersion relation, indicating that the frequency dispersion term $\varepsilon_{fr}(f)$ and the amplitude dispersion term $\varepsilon_{am}(f)$ in Eq. 3 are of almost equal magnitude and cancel, yielding a nondispersive wave field in which all components travel with the shallow water wave speed $(gh)^{1/2}$.

Case III. OCTOBER 19

The October 19 case (Fig. 6), the most energetic of the four cases, was collected at the height of a severe nor'easter storm with strong winds from the north (speeds up to 18 m/s). The offshore significant wave height was 3.64 m, with a mean propagation direction about 10° north of normal incidence. The observed spectra are characterized by a narrow peak centered at $f_p \approx 0.1$ Hz, accompanied by a pronounced 2nd harmonic peak at $2f_p \approx 0.2$ Hz (Fig. 6a). Wave breaking is again evident in the strong attenuation of spectral levels. Observed swell variances decreased by about 32% between the offshore buoy and array 7, 45% between arrays 7 and 6, and by 50% between arrays 6 and 5 (Fig. 6a), indicating that all arrays are located well inside the surf zone. There is still excellent agreement between the observed $k_{rms}(f)$ and the linear finite depth dispersion relation at the spectral peak frequency, but at f_p the observed $k_{rms}(f)$ are consistently smaller than the linear wavenumber. At the highest frequency (0.25 Hz) the discrepancies at the deeper arrays (6, 7) exceed 30% (Figs. 6c, d). Note that at arrays 6 and 7 the nonlinear

14

predictions of $k_{rms}(f)$ exceed $k_{sw}(f)$ at high frequencies, that is, high-frequency

components travel with a speed slightly faster than the $(gh)^{1/2}$ speed of the spectral peak

components (Fig. 6c). The nonlinear Boussinesq predictions generally agree well with

the observed wavenumbers, but tend to slightly over-predict the observed wavenumbers

at higher frequencies. Similar to Case II, the nonlinear Boussinesq prediction of $k_{rms}(f)$

is close to the shallow water dispersion relation, indicating canceling frequency and

amplitude dispersion effects.

Case IV. SEPTEMBER 4

On September 4 during a short-lived but intense storm a broad spectrum of

energetic, relatively high frequency seas ($f_p \approx 0.15$ Hz) were observed (Fig. 7). Wind was

from the north with speeds up to 14 m/s. The offshore significant wave height was 2.38

m, with an oblique mean wave direction of about 38° north of normal incidence.

Observed variances decreased by 30% between arrays 7 and 6 and by 40% between the

arrays 6 and 5, again indicating a wide surf zone that spans the instrumented region (Fig.

7a). As in the previous case studies, there are large discrepancies between the observed

$k_{rms}(f)$ and the linear finite depth dispersion relation, which tends to over-predict the

wavenumber most notably at high frequencies (Figs. 7b-d). In contrast to the other

studies, the nonlinear Boussinesq model prediction is in poor agreement with the

observed $k_{rms}(f)$ at high frequencies. The nonlinear and linear Boussinesq predictions

are nearly equal, indicating that the predicted amplitude dispersion is weak. The failure

of the nonlinear Boussinesq model to predict the observed large deviations of $k_{rms}(f)$

15

from the linear dispersion relation in this case may be explained by the relatively high spectral peak frequency. The Boussinesq approximation is formally valid only for $kh \ll 1$ while observed values of $k_{rms}(f_p)h$ vary between 0.5 and 0.7. The observed small $k_{rms}(f)$ at high frequencies suggest that the high-frequency tail of the spectrum is dominated by bound waves generated in non-resonant sum, triad-interactions (e.g. Herbers & Guza, 1994).

Interestingly, at frequencies below f_p, the observed $k_{rms}(f)$ at the deeper arrays (6, 7) are about 5-20% higher than the linear wavenumber (Figs. 7c, d). The same tendency, although less pronounced, is also present in the nonlinear Boussinesq prediction. These larger wavenumbers and the observed enhancement of low frequency spectral levels between arrays 7 and 4 (Fig. 7a) are qualitatively consistent with theoretically expected nonlinear energy transfers in difference triad interactions from the spectral peak to lower frequency bound waves (e.g. Herbers et al., 1994).

IV.   ACCURACY OF LINEAR AND NONLINEAR MODELS

The limited validity of the linear finite depth dispersion relation in shallow water and the improved accuracy of wavenumbers predicted by a Boussinesq model that accounts for nonlinear amplitude dispersion effects are evaluated here through comparisons with observed wavenumbers for the entire data set. In order to examine the accuracy of the models in relation to incident wave conditions, the data for each array were binned in 10 equal log-spaced classes of wave variance. For each class the mean and standard deviations were computed of the ratio between the observed and predicted wavenumber $k_{rms}(f)$ (at a fixed frequency f). Results for all four arrays at the peak frequency f_p and harmonic frequencies $2 f_p$ and $3 f_p$ are shown in Figs. 8 –11, with predicted $k_{rms}(f)$ based on the linear dispersion relation (left panel) and the nonlinear Boussinesq model (right panels).

At the peak frequency f_p, the linear and nonlinear predictions agree about equally well with observations. The bias is small (i.e. the mean observed/predicted ratio is close to 1) and increases only very slightly with increasing variance for the linear model. These comparisons show that amplitude dispersion effects are weak at the spectral peak frequency. For both the linear and nonlinear models, the standard deviation of observed/predicted wavenumbers are larger at arrays 4 and 5 (close to shore) than at arrays 6 and 7 (farther from shore), and appears to decrease with increasing wave variance (Figs. 10a, b; 11a, b). As discussed in Chapter III, a likely cause of this scatter

17

are errors in observed wavenumbers caused by partial standing wave patterns that are most pronounced for smaller amplitude waves closer to shore.

At the harmonic frequencies $2f_p$ and $3f_p$, marked differences are noted between the performance of linear and nonlinear models. The nonlinear model predictions of $k_{rms}(2f_p)$ and $k_{rms}(3f_p)$ have very small bias (less than a few percent) and low scatter (Figs. 8 - 11, panels d, f). Although small, the discrepancies (both bias and scatter) are notably larger for array 6 (Fig. 9d, f) than for the other three arrays. Possibly the observed wavenumbers at high frequencies at array 6 are degraded by unknown errors in the sensor positions (surveyed from shore while the instrument frames were jetted in the bottom).

The importance of amplitude dispersion at high frequencies is evident in the large discrepancies (up to 40%) between the observed $k_{rms}(2f_p)$ and $k_{rms}(3f_p)$ and the linear wavenumber predictions (Figs. 8 – 11, panels c, e). At all four arrays the linear wavenumber is consistently larger than the observed wavenumber, and this bias increases with both increasing frequency and increasing wave variance.

The overall agreement of observed and predicted wavenumbers is summarized in Fig. 12. An observed energy weighted root-mean square wavenumber k_{rms}

$$k_{rms} = \left(\frac{\int_{0.05\,Hz}^{0.25} k_{rms}^2(f)E(f)df}{\int_{0.05\,Hz}^{0.25} E(f)df} \right)^{1/2} \tag{7}$$

18

is compared to bulk k_{rms} predictions based on the linear finite depth dispersion relation

(Fig. 12a, c, e, g) and the nonlinear Boussinesq model (Fig.12b, d, f, h). The linear

wavenumbers are consistently biased high. For low energy conditions, the bias is less

than 10% at all arrays. For high energy conditions the bias varies between 10% at array 4

to about 20% at the deeper arrays 6 and 7. The nonlinear Boussinesq predictions have

biases less than 5% that do not vary with variance levels. Interestingly, the bias and

scatter in the nonlinear model comparisons varies between the four arrays from very

small values (a few percent) at array 5 to more significant discrepancies (O(5%)) at array

6. These differences that appear to be insensitive to incident wave conditions are, as

mentioned earlier, possibly the result of small errors in the observed wavenumbers

resulting from uncertainties in the sensor positions. Overall, results of the present study

show that wave nonlinearity in shallow water causes significant (O(20%)) deviations

from the linear dispersion relation, and that these amplitude dispersion effects are

described accurately by a weakly nonlinear Boussinesq model.

V. SUMMARY

Nonlinear effects on the dispersion relation of waves in shallow water were examined with measurements collected on a sandy beach at the U.S. Army Corps of Engineer's Field Research Facility during the recent SandyDuck experiment. The barrier island field site is characterized by a straight coastline with a gently sloping, nearly planar, inner shelf and beach. Four arrays of bottom pressure sensors were deployed in depths ranging from 3 – 6 m during August-November, 1997 (Fig. 1).

A detailed analysis is presented of wavenumbers observed at the four arrays in four one-hour-long case studies that were taken from major storms as well as a calm period, and span the range of conditions encountered during the four month long experiment (Fig. 3 - 7). A root-mean-square average wavenumber $k_{rms}(f)$ was estimated as a function of frequency (Eq. 6) from the array cross-spectra. These estimates are compared with the linear finite depth dispersion relation (Eq. 1) and a nonlinear theory prediction of $k_{rms}(f)$ based on Boussinesq equations. In the latter model, $k_{rms}(f)$ is given by the shallow water dispersion relation with 2nd order correction terms that account for the competing effects of frequency dispersion (i.e. decrease in wave speed with increasing frequency) and amplitude dispersion (i.e. increase in wave speed with increasing amplitude) (Eq. 3). The observed wavenumbers are generally in excellent agreement with the nonlinear theory predictions over a wide frequency range. In low energy conditions, amplitude dispersion is weak and the observed wavenumbers remain

21

close to the linear dispersion relation, consistent with the model predictions (Fig. 4). In high-energy conditions with actively breaking or nearly breaking waves, amplitude dispersion causes significant deviations from the linear dispersion relation. The effects of amplitude and frequency dispersion tend to cancel and as a result all components of the wave spectrum travel with approximately the shallow water wave speed $\sqrt{gh}$ (Figs 5, 6). In some cases with steep high-frequency seas, deviations from the linear dispersion relation are larger than those predicted by the Boussinesq model (Fig. 7), possibly because the Boussinesq shallow water approximation is violated.

Analysis of the entire data set shows systematic deviations from the linear finite depth dispersion relation that increase with both increasing frequency and increasing total wave energy (Figs. 8 – 12). Wheras the linear dispersion relation overpredicts wavenumbers of high-frequency wave components by as much as 20-40%, the nonlinear Boussinesq model predictions are typically within ±5% of the observed wavenumbers.

APPENDIX

Figure 1. Plan view of the four bottom pressure sensor arrays (numbered 4 –7) used in this study. Filled circles represent all sensor locations. Associated depth contours (relative to mean sea level) at 1 m intervals (based on a survey conducted on 16 September 97 are indicated by dotted lines.

Figure 2. Detailed plan view of the four bottom pressure sensor arrays.

Figure 3. Wave variance observed at the four arrays versus time for the duration of the entire experiment. The four case studies analyzed in Figs. 4 –7 are indicated with vertical dotted lines.

Figure 4. Comparison of observed and predicted wavenumbers for case I data collected on 20 November, 02:00 – 03:00 EST. (a) Observed wave pressure spectra $(E(f))$ at each array. The corresponding wave variances (in the range of 0.05 – 0.25 Hz) are indicated. (b –d) For each array, the observed root-mean-square average wavenumber, as a function of frequency $k_{rms}(f)$ (asterisks) is compared to predictions based on the linear finite depth dispersion relation (solid line, Eq. 1) and the nonlinear Boussinesq model (circles, Eq. 3). Also included are the linear shallow water dispersion relation (dotted line) and the dispersion relation of the linearized Boussinesq model (dash-dotted line).

Figure 5. Comparison of observed and predicted wavenumbers for case II data collected on 7 November 02:00 – 03:00 EST (same format as in Fig. 4).

Figure 6. Comparison of observed and predicted wavenumbers for case III data collected on 19 October 16:00 – 17:00 EST (same format as in Fig. 4).

Figure 7. Comparison of observed and predicted wavenumbers for case IV data collected on 4 September 02:00 – 03:00 EST (same format as in Fig. 4).

Figure 8. Comparison at array 7 of observed and predicted $k_{rms}(f)$ at the peak frequency f_p (upper panels) and the harmonic frequencies $2f_p$ (middle panels) and $3f_p$ (lower panels). The ratio between the linear finite wavenumber and the observed wavenumber (left panels), and the ratio between the nonlinear Boussinesq wavenumber and the observed wavenumber $k_{rms}(f)$ (right panels) are shown versus total wave variance. The data are binned in 10 equal log-spaced classes of wave variance containing between 12 and 534 data records. Each vertical bar represents the mean and ± one standard deviation of the ratio data.

Figure 9. Comparison at array 6 of observed and predicted $k_{rms}(f)$ at frequencies f_p, $2f_p$, $3f_p$ records collected with same format as in Fig. 8, (each bar represents between 8 and 417 data records).

Figure 10. Comparison at array 5 of observed and predicted $k_{rms}(f)$ at frequencies f_p, $2f_p$, $3f_p$ records collected with same format as in Fig. 8, (each bar represents between 20 and 453 data records).

Figure 11. Comparison at array 4 of observed and predicted $k_{rms}(f)$ at frequencies f_p, $2f_p$, $3f_p$ records collected with same format as in Fig. 8, (each bar represents between 18 and 381 data records).

Figure 12. Comparison of observed and predicted the bulk k_{rms} (Eq. 7) at all four arrays. The ratio between the linear finite depth prediction and the observed k_{rms} (left panels), and the ratio between the nonlinear Boussinesq prediction and the observed k_{rms} (right panels) are shown versus total wave variance. The data are binned in 10 equal log-spaced classes of wave variance containing between 21 and 534 data records. Each vertical bar represents the mean and ± one standard deviation of the ratio data.
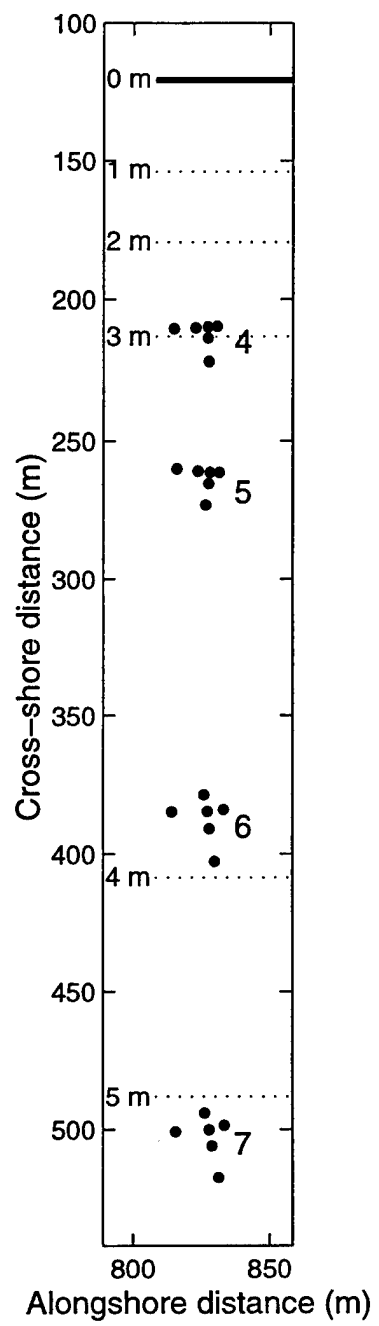
Figure 1
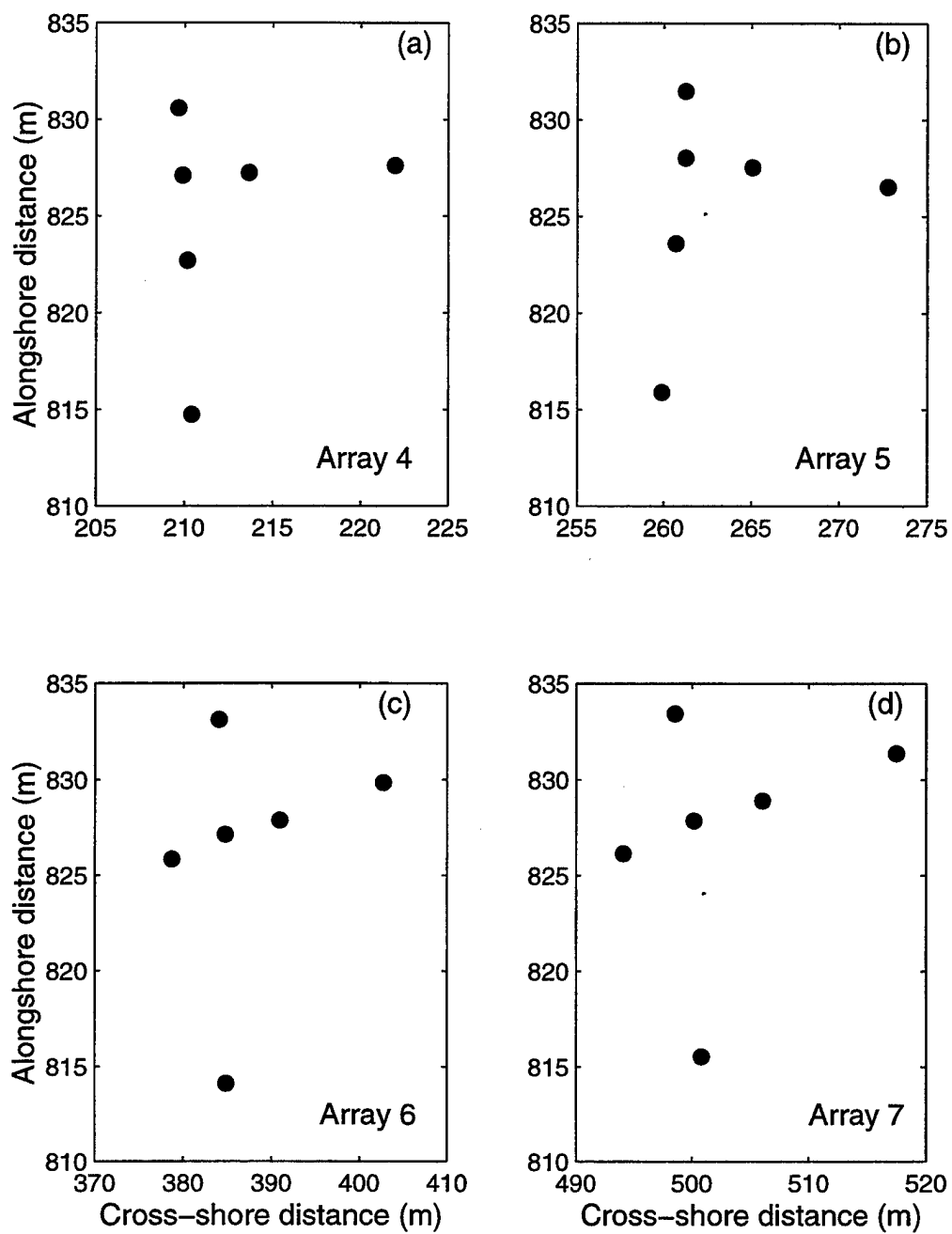
Figure 2
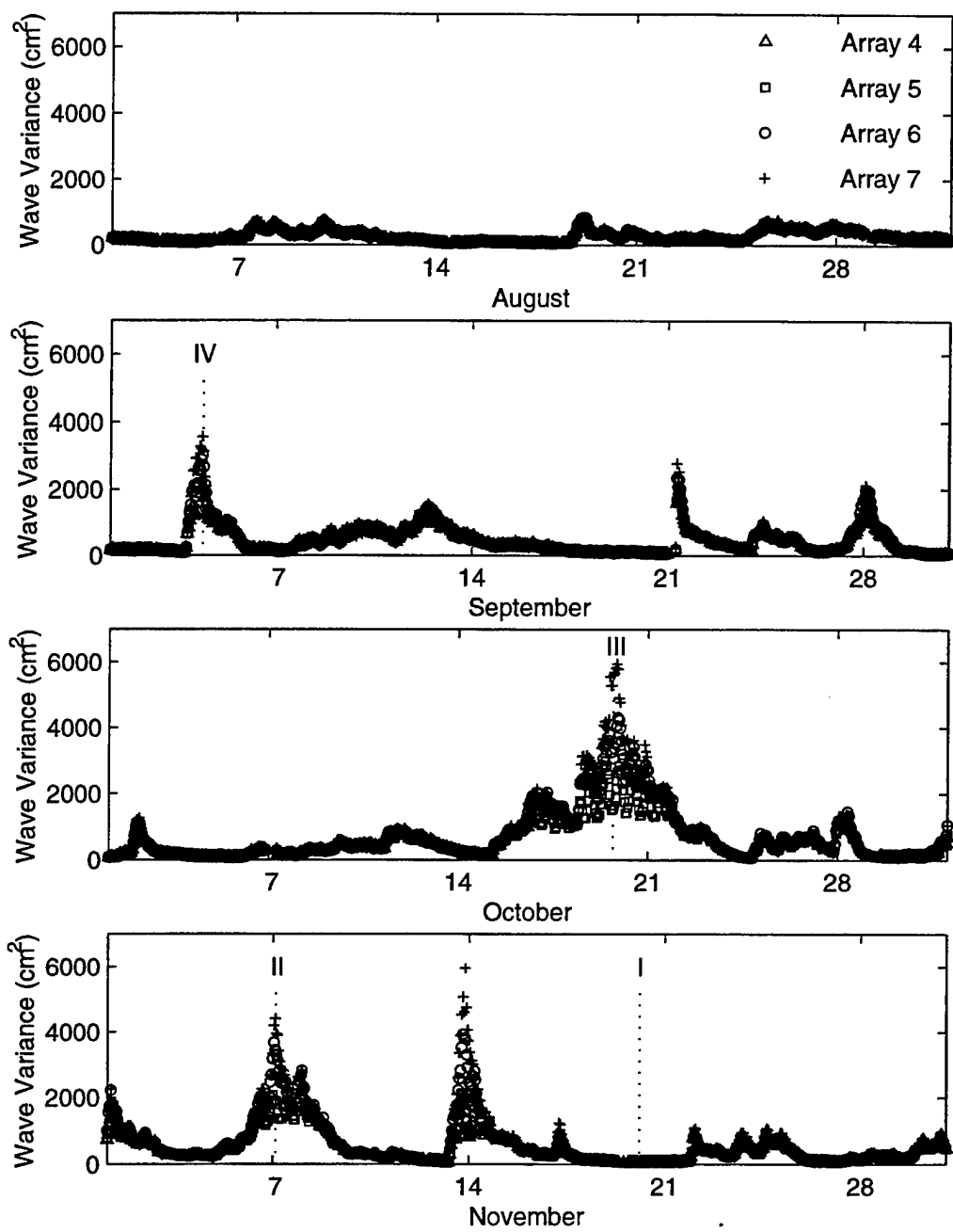
Figure 3
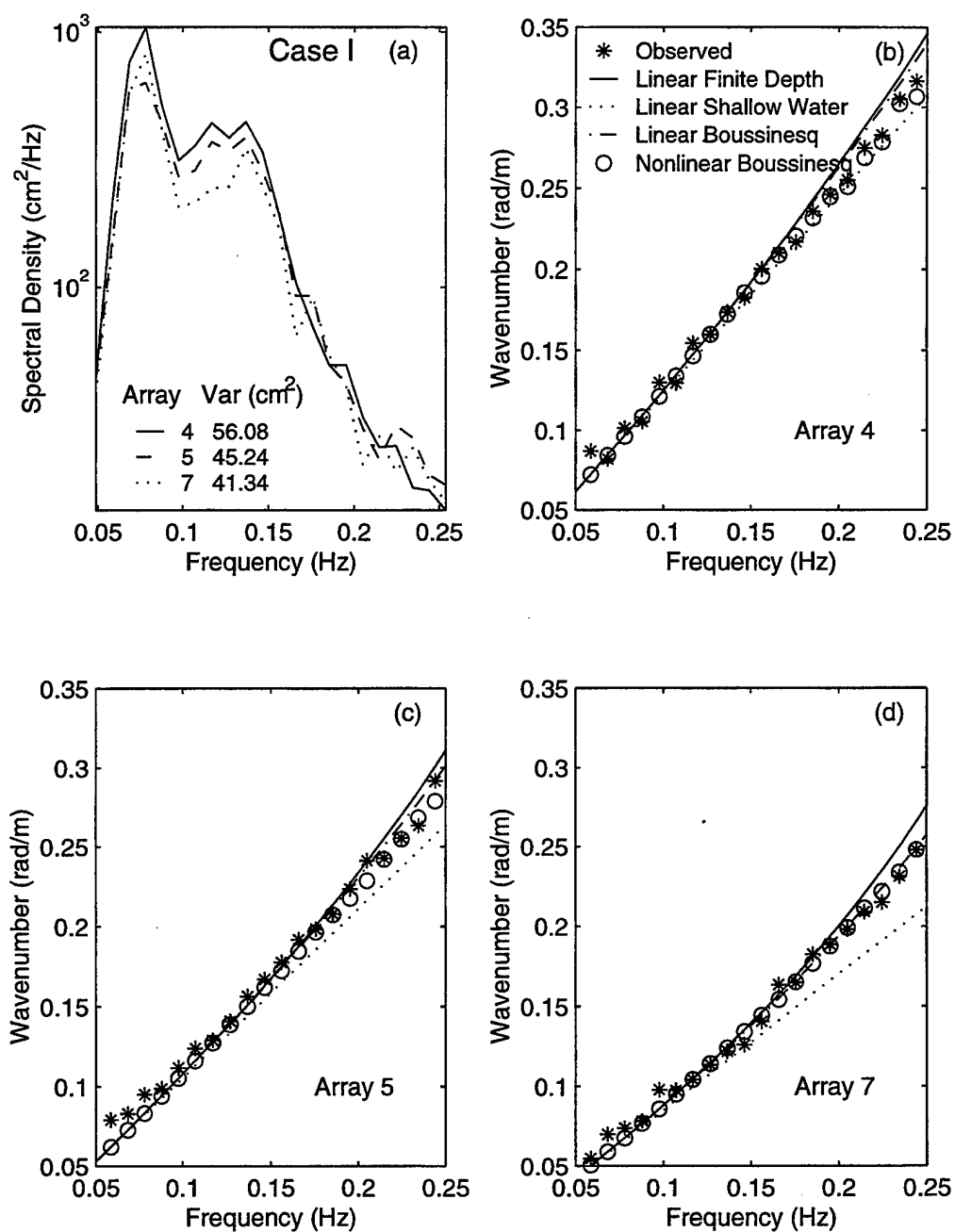
Figure 4

Figure 5

Figure 6

31

Figure 7

Figure 8

33
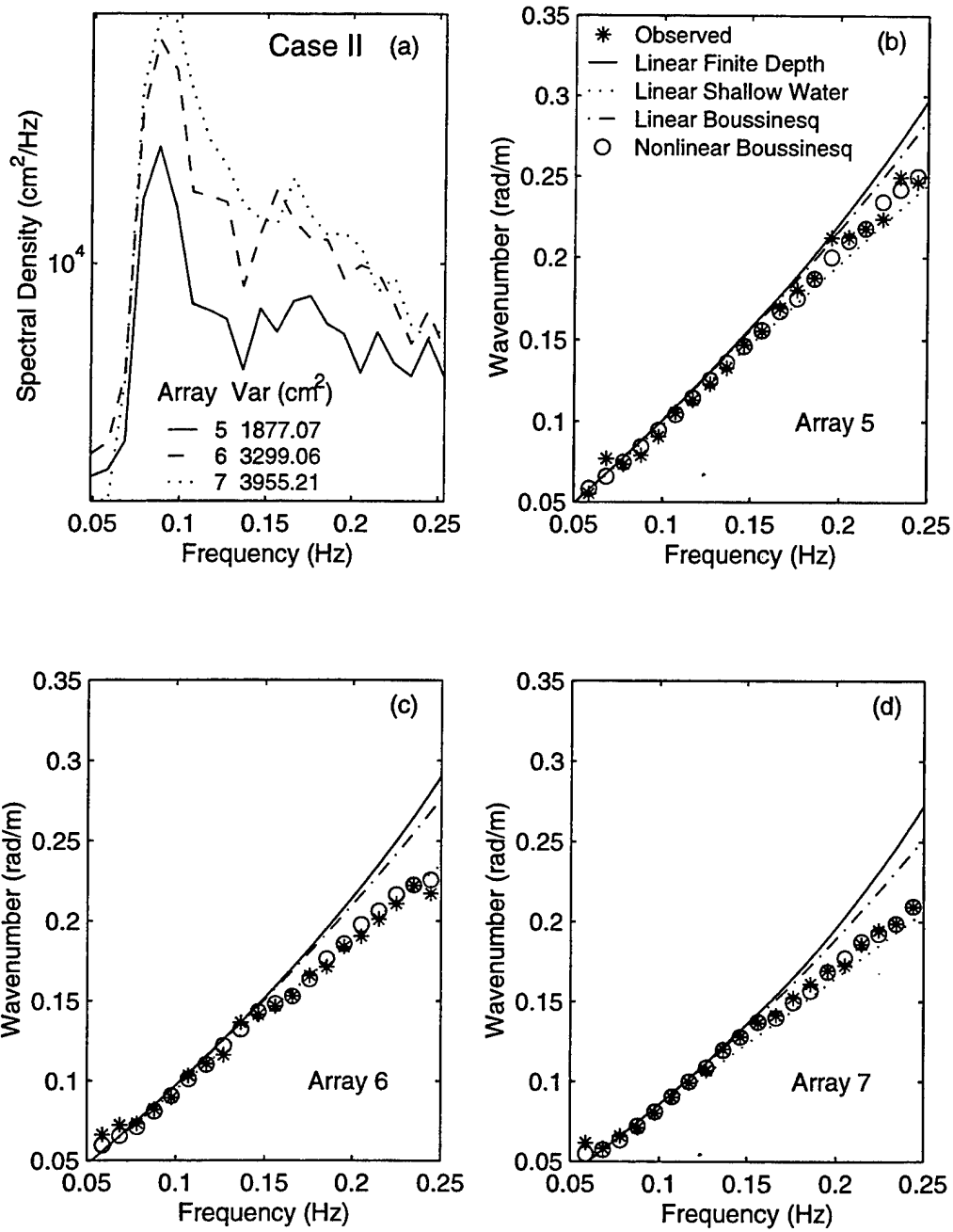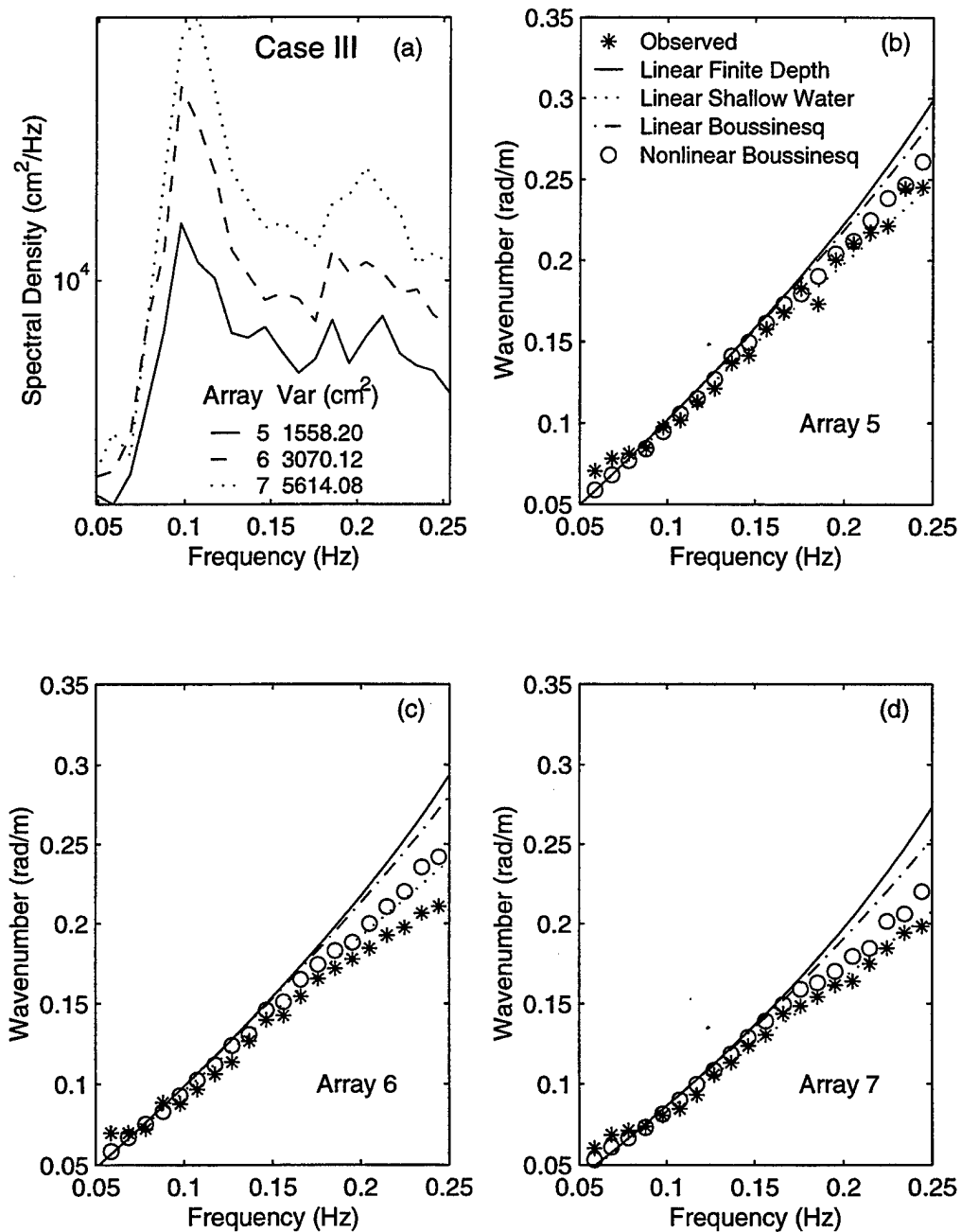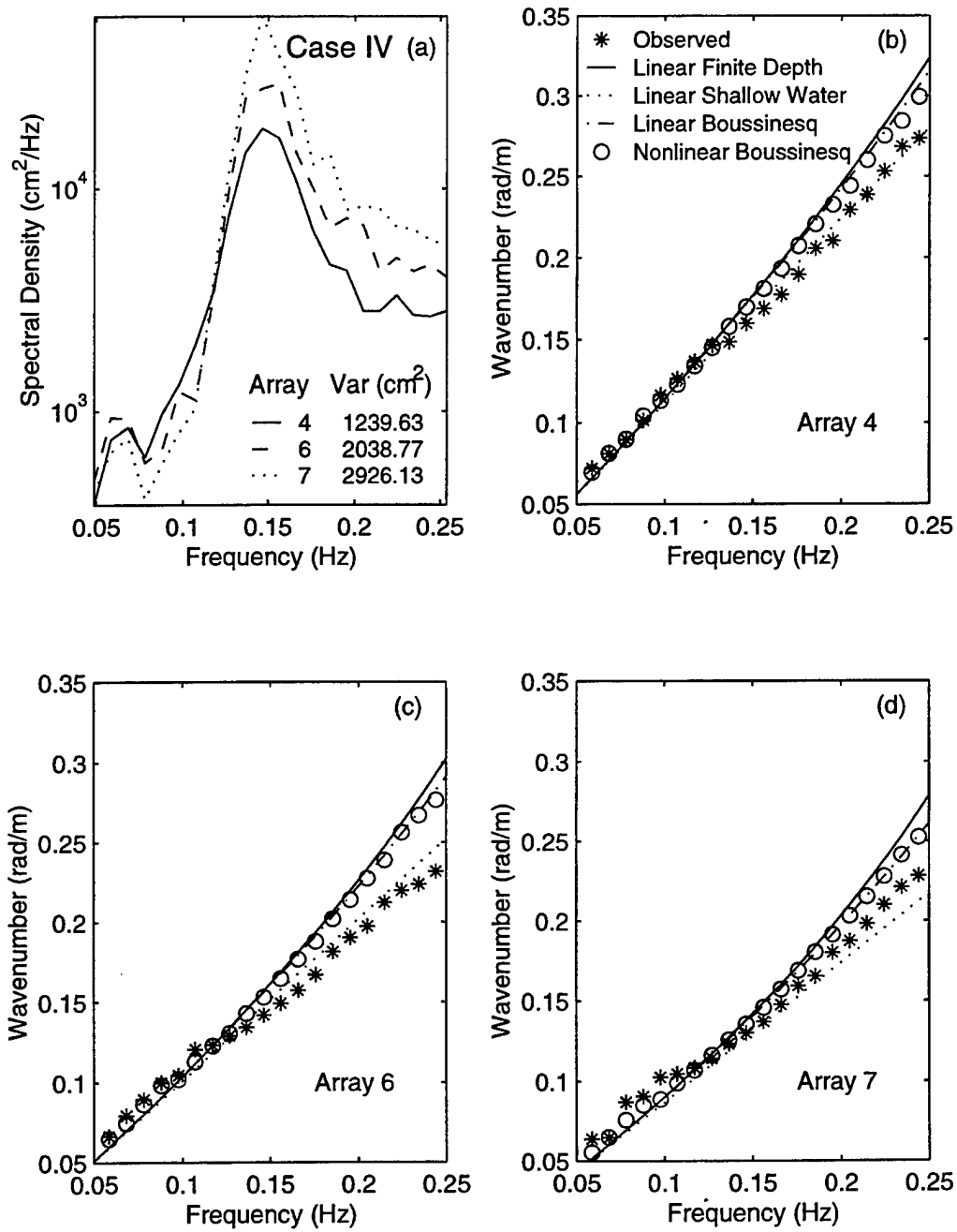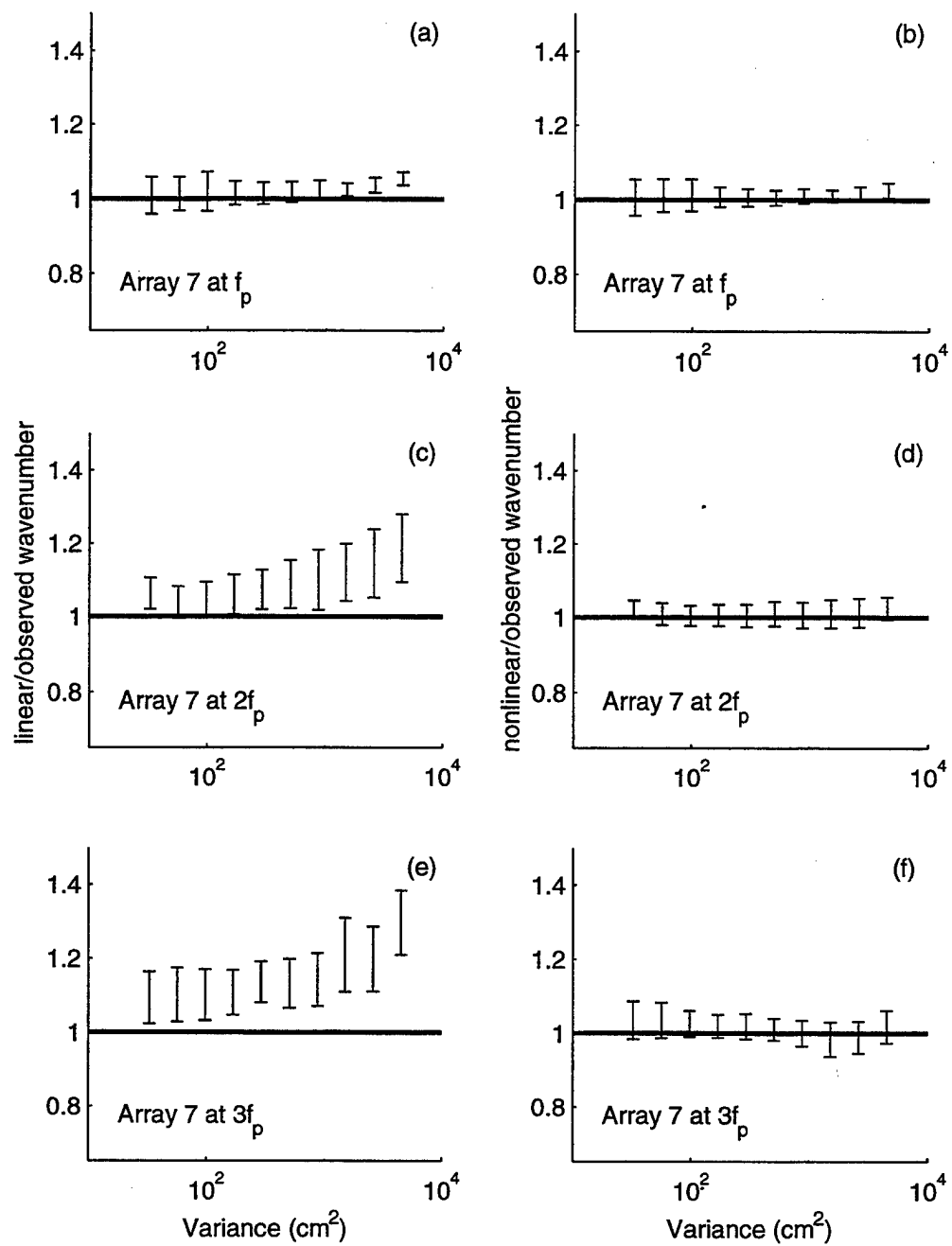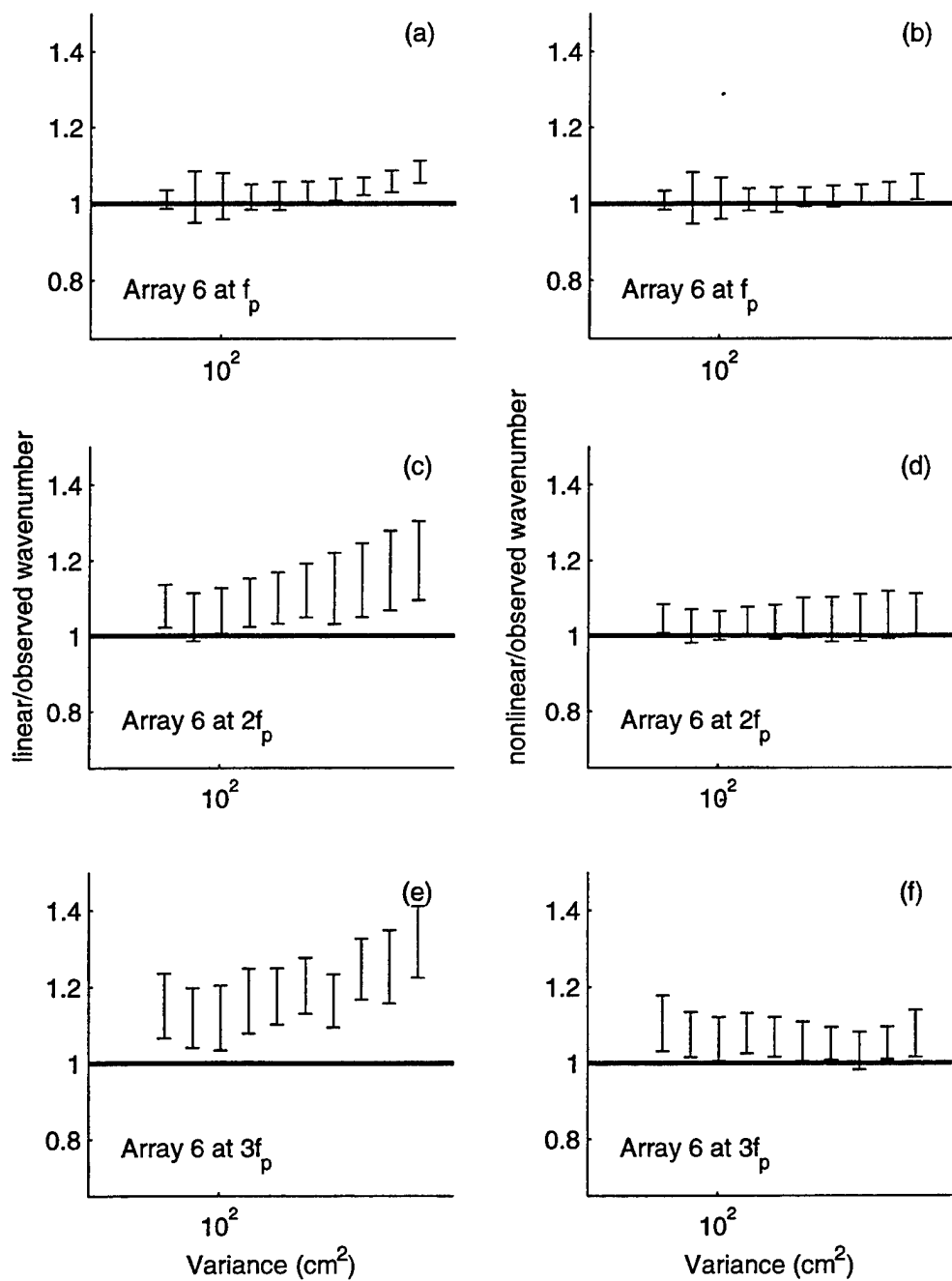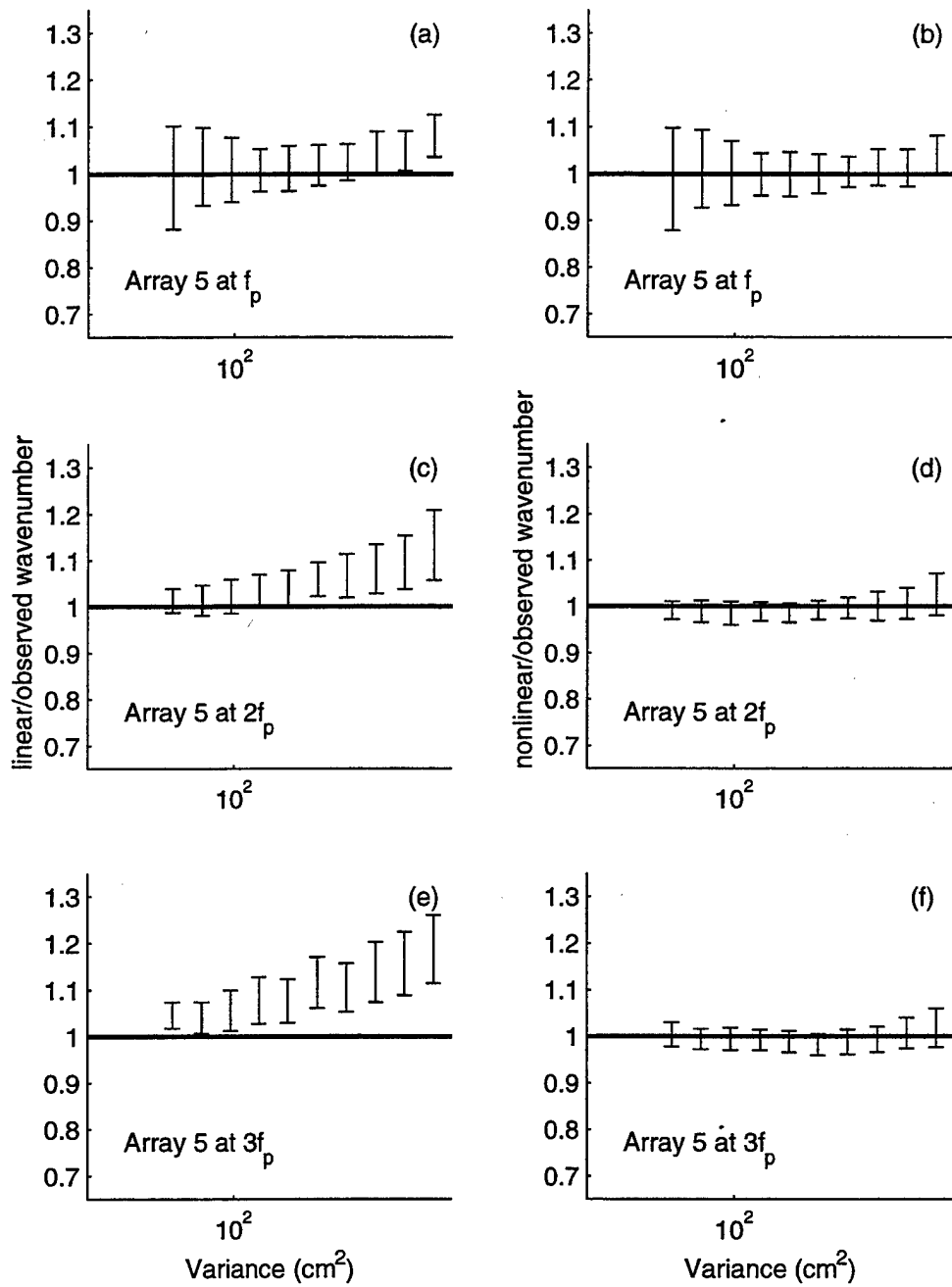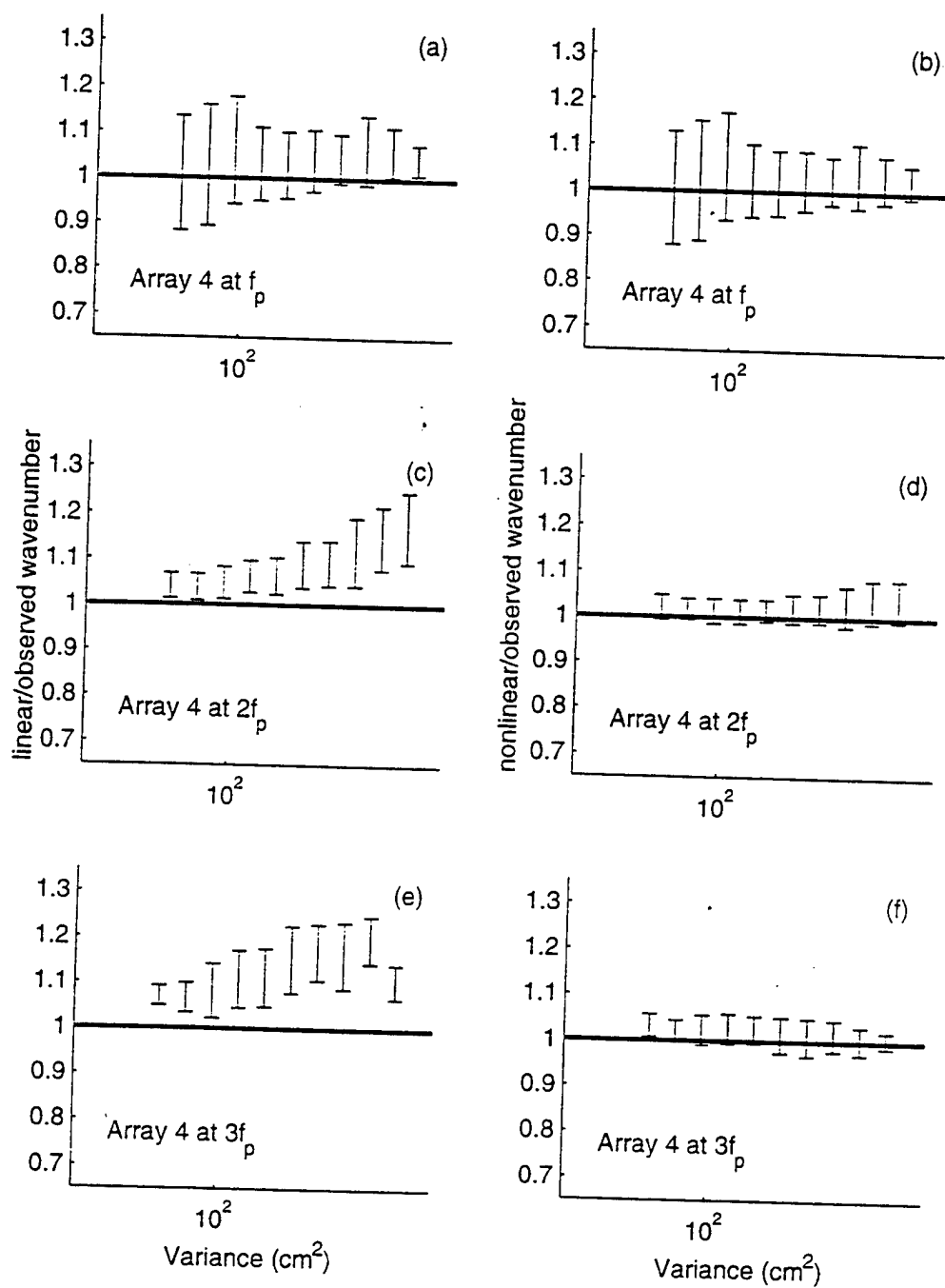
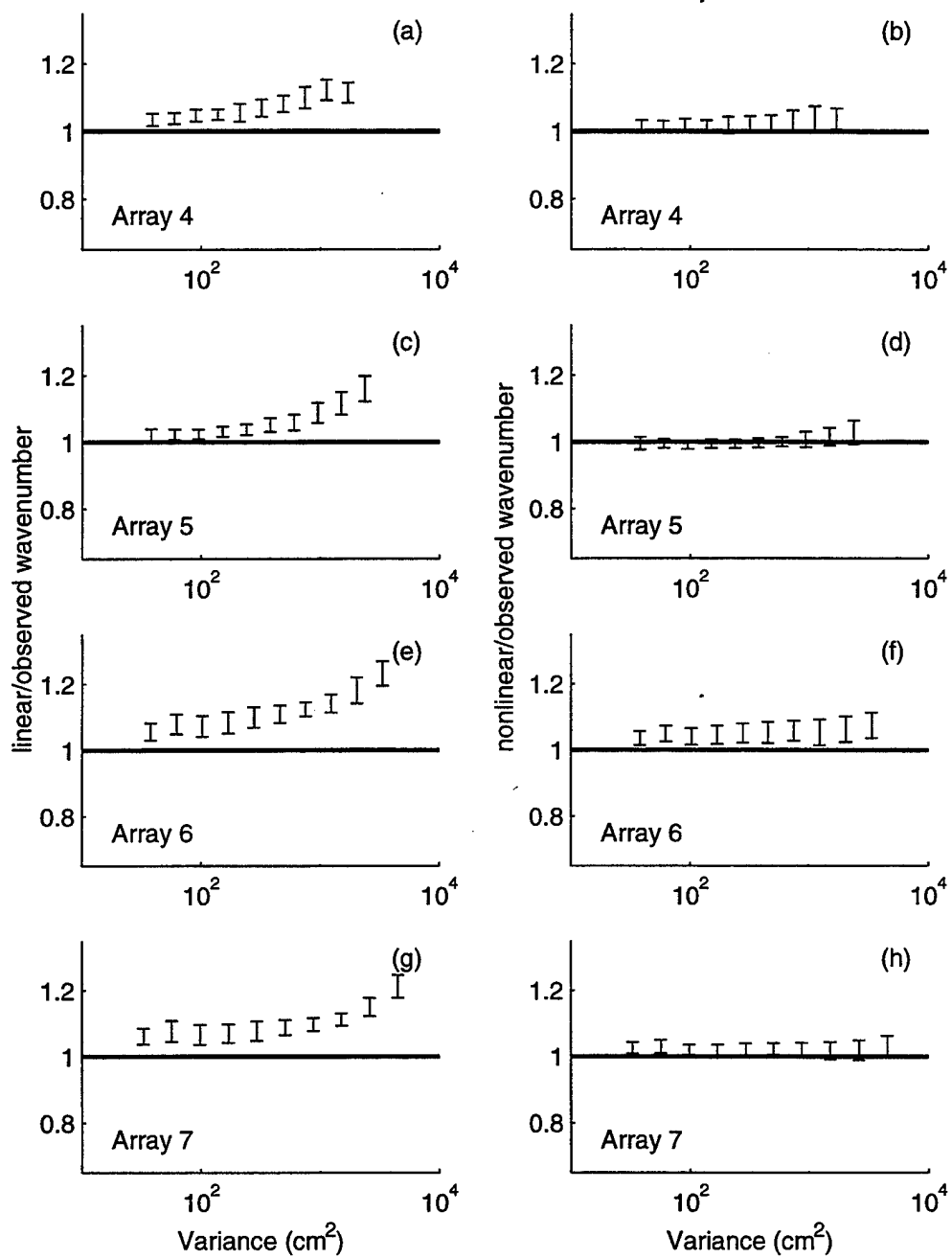**Figure 9**

Figure 10

Figure 11

Figure 12

LIST OF REFERENCES

Donelan, M. A., J. Hamilton, and W. H. Hui, 1985: Directional Spectra of wind-generated waves. *Phil. Trans. R. Soc. Lond., A315, 509-562.*

Elgar, S., and R. T. Guza, 1985: Shoaling gravity waves: comparisons between field observations, linear theory, and a nonlinear model. *J. Fluid Mech., 158,* 47-70.

Elgar, S., T. H. C. Herbers, and R. T. Guza, 1994: Reflection of ocean surface gravity waves from a natural beach. *J. Phys. Oceanogr., 24(7), 1503-151* 1.

Freilich, M. H., and R. T. Guza, 1984: Nonlinear effects on shoaling surface gravity waves. *Phil. Trans. R. Soc. Lond., A3J1, 1-41.*

Herbers, T. H. C., and R. T. Guza, 1992: Wind-wave nonlinearity observed at the sea floor, Part II: Wavenumbers and third-order statistics, *J. Phys. Oceanogr,.* 22(5), 489-504.

Herbers, T. H. C., R. L. Lowe, and R. T. Guza, 1992: Field observations of orbital velocities and pressure in weakly nonlinear surface gravity waves. *J. Fluid Mech., 245,* 413-435.

Herbers, T. H. C., S. Elgar, and R. T. Guza, 1994: Infragravity-frequency (0.005-0.05 Hz) motions on the shelf, Part 1: Forced waves. *J. Phys. Oceanogr., 24,* 917-927.

Herbers,.T. H. C., and R. T. Guza, 1994: Nonlinear wave interactions and high-frequency seafloor pressure, *J. Geophys. Res.,* 99(C5), 10035-10048, 1994.

Herbers, T. H. C., and M. C. Burton, 1997: Nonlinear shoaling of directionally spread waves on a beach. *J. Geophys. Res., 102,* 21101-21114.

Herbers, T. H. C., S. Elgar, and R. T. Guza, 1995: Generation and propagation of infragravity waves. J. *Geophys. Res.,* 100, 24863-24872.

Herbers, T. H. C., S. Elgar, R. T. Guza, and W. C. O'Reilly, 1995b: Infragravity-frequency (0.005-0.05 Hz) motions on the shelf, Part II: Free waves. *J. Phys. Oceanogr., 25,* 1063-1079.

Kinsman, B., 1965, "Wind waves: Their generation and propagation on the ocean surface", Prentice Hall, Englewood Cliffs, N.J. 676 pp.

Peregrine, D. H., 1967: Long waves on a beach. *J. Fluid Mech. 27,* 815-827.

INITIAL DISTRIBUTION LIST